

Jet Formation and Collimation in AGN and μ -Quasars

Christophe Sauty¹, Kanaris Tsinganos², and Edoardo Trussconi³

¹ Université Paris 7 - Observatoire de Paris, D.A.E.C., F-92190 Meudon, France

² Department of Physics, University of Crete, GR-710 03 Heraklion, Crete, Greece.

³ Osservatorio Astron. di Torino, Strada Osservatorio 20, I-10025 Pino Torinese, Italy

Abstract. We briefly review our current understanding for the formation, acceleration and collimation of winds to jets associated with compact astrophysical objects such as AGN and μ Quasars.

All such outflows may be considered to a first approximation as ideal MHD plasmas escaping from a rotating and magnetized accretion disk with a magnetosphere around a central black hole. A crucial ingredient for a correct modelling of the steady state problem is to place the appropriate boundary conditions, by taking into account how information can propagate through the outflow and ensuring, e.g., that shocks produced via the interaction of the flow with the external medium do not affect the overall structure. As an example underlining the role of setting the correct boundary conditions, we make the analogy of the critical surfaces in the steady and axisymmetric MHD problem with the event horizon and ergosphere of a rotating black hole in relativity.

We discuss the acceleration of the outflow, by gas, radiation, or wave pressure gradients and also by magnetic mechanisms, showing the important role played by the disk corona in the vicinity of the black hole. Pressure and magnetic confinement both may also play a role in confining the outflow, although magnetic hoop stress confinement is likely to be a rather dominant process in tightly collimated outflows. The possible asymptotical morphology that jets achieve and the instabilities which are likely to explain the observed structures but do not prevent jets to possess toroidal magnetic fields are also reviewed.

Finally, it is proposed that in a space where the two main variables are the energy of the magnetic rotator and the angle between the line of sight and the ejection axis, some observed characteristics of AGN jets can be understood. A criterion for the transition of the morphologies of the outflows from highly collimated jets to uncollimated winds is given. It is based on the analysis of a particular class of exact solutions and may somehow generalize other earlier suggestions, such as the spinning of the black hole, the fueling of the central object, or the effects of the environment.

Thus, while the horizontal AGN classification from Type 0 to Types 1 and 2 may well be an orientation effect – i.e. a dependence on the viewing angle between the source axis and the observer as in the standard model – the vertical AGN classification with uncollimated outflows (radio-quiet sources) and collimated outflows (radio-loud sources) depends both, on the efficiency of the magnetic rotator and the environment in which the outflows propagate.

1 Introduction

1.1 Schematic picture of AGN

Some galaxies are known to emit radiation with extremely high luminosities from rather small volume in the γ -ray, X-ray and UV continuum. Such active cores are the so-called Active Galactic Nuclei (AGN) and the radiation is commonly believed to be gravitational energy released by matter spiraling around a supermassive central black hole of about $10^9 M_\odot$ (see Fig. 1).

Though the central engine which produces the enormous observed activity cannot be resolved observationally, a standard picture of an AGN has gradually emerged to explain the richness of the radiation spectra:

- an accretion disk from about 2 to 100 gravitational radii, R_g , feeding the central black hole and emitting mainly in the UV and soft X-rays;
- the broad line optically emitting clouds (BLR), which seem to be absent in some sources (e.g. FRI, see hereafter) and extend up to a few $10^3 R_g$ from the center. The BLR emission can be radiation scattered by hot electrons further away while the word “cloud” should be taken in the broad sense meaning dense gas with a filling factor less than unity [77];
- a dusty torus (or wrapped disk or dusty bipolar flow) with an inner radius of a few $10^3 R_g$, which obscures the central parts of the AGN from transverse lines of sight;
- the narrow line regions (NLR) which extend from about 10^4 to $10^6 R_g$;

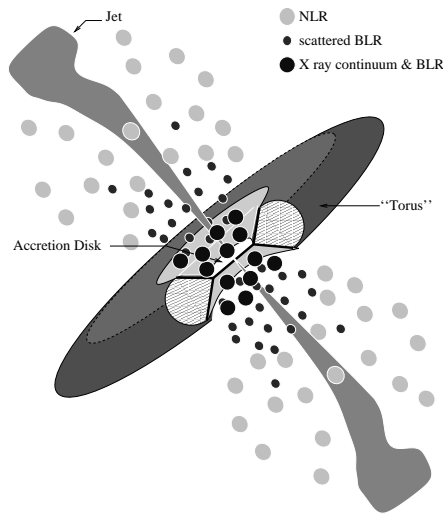


Fig. 1. General sketch, not to scale, of an AGN following Urry and Padovani ([98], see the text for details).

- powerful jets of plasma detected from the sub-parsec to the Mpc scales, mainly in the radio but also in the optical, UV and X-rays.

Note also, that ultra high energy γ -rays have also been observed from the central regions of several Blazars. Jets, together with the emission of radiation from the immediate neighborhood of an AGN provide a crucial link between the easier observed large Mpc scale and the sub-parsec scales where presumably the plasma of the jets is accelerated in a few gravitational radii from the center of the AGN.

1.2 Unified Schemes for AGN

Based on the phenomenology of their emission in the radio and optical/UV parts of the spectrum, AGN are commonly divided into three broad classes, as it may be found in excellent reviews in [1,98]. Although some details have been already modified since then, the overall classification still holds nowadays, at least as far as the properties of the associated winds and jets are concerned:

- Type 2 AGN have weak continua with narrow emission lines (NLR). They include, in the radio quiet group, the low luminosity Seyfert 2 galaxies and narrow emission line galaxies (NELG) while the radio-loud counterpart regroups the narrow-line radio galaxies with the two distinct morphologies of Fanaroff-Riley I (low-luminosities, FR I) and Fanaroff-Riley II (higher luminosities, FR II).

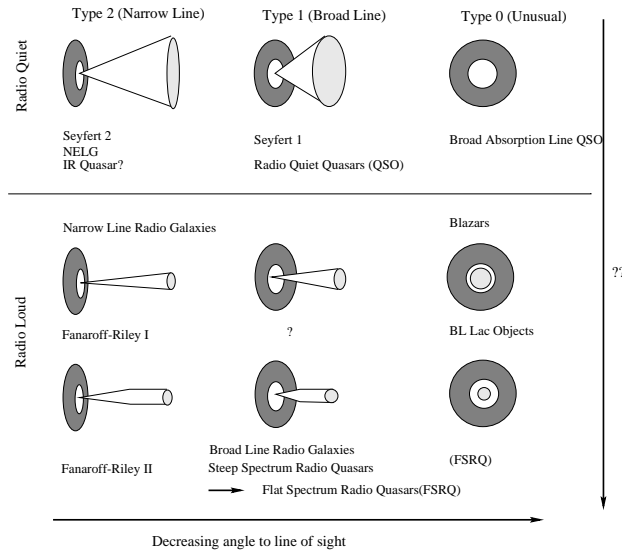


Fig. 2. Unified scheme presented by Urry and Padovani 1995 ([98]). Properties of AGN depend on at least two parameters: the viewing angle and some other parameter yet to be defined.

- Type 1 AGN have bright continua with broad emission lines (BLR) in addition to the NLR. The type 1 radio-quiet group is composed of the low luminosity Seyfert 1 galaxies (Sey 1) and the higher luminosity radio-quiet quasars (QSO), while the radio-loud group includes the broad line radio galaxies (BLRG) at low luminosities and the flat or steep spectrum radio-loud quasars (FSRQ and SSRQ) at higher luminosities.
- Type 0 AGN correspond to the remaining AGN with weak or unusual emission lines, i.e., in the radio-quiet end the broad absorption lines QSO (BALs) and in the radio-loud end the Blazars (BL Lacs and flat spectrum radio quasars, FSRQ).

Thus, the various AGN can be classified according to orientation, beaming and obscuration effects [98]. In this classification scheme, the transition from Type 0 to Type 1 and then to Type 2 of the class of radio-quiet AGN is based on orientation effects alone (Fig. 2). Namely, in Type 0 AGN the line of sight is almost coincident with the axis of the system, while the disk is seen face-on. In Type 2 the viewing angle is close to 90° (disk edge-on) and obtains intermediate values for Types 1. The broad emission lines arise from “clouds” (i.e. dense gas with a small filling factor) orbiting above but nearby the disk (Fig. 1). Thus when the line of sight makes a small angle with the system axis, they are not obscured by the dusty torus, as in Seyfert 1, while wherein these broad emission lines are obscured by the torus, only the narrow emission lines are visible because they are produced further away, as it is the case with Seyfert 2.

Similarly among radio-loud galaxies, the transition from Type 0 (Blazars) to Type 2 (FR I/II radio galaxies) is based on a combination of orientation with relativistic beaming, i.e., whether a radio-loud AGN is a radio galaxy or a Blazar, and also depends on the angle between its relativistic jet and the line of sight. In this sense there seems to be a transition from FSRQ (Type 0) to SSRQ (Type 1) and then FR II (Type 2). For low luminosity radio loud galaxies there seems to be a gap as BL Lac objects (Type 0) are associated with FR I (Type 2) with no Type 1 counterpart. Although this association is still controversial, it may be explained by an intrinsic absence of broad emission line clouds [28] which would prevent to find any corresponding Type 1 objects with a BLR. This argument is supported by the fact that with increasing resolution BLR are also sometimes detected in FR II. At the same time however, recent data at optical and X-ray wavelengths have shown that, for the FR I/BL Lac case, the standard unification model does not seem to be in full agreement with observations. A possible way out to reconcile observations with the standard unification scheme is to assume a structure of the velocity across the jet ([21,29]).

It is now clear that orientation effects are not sufficient to explain the difference between radio-quiet, low luminosity and radio loud and high luminosity galaxies and quasars. It seems that in radio-loud AGN the outflow is relativistic at least in parsec scales, very well collimated in the form of a jet

and quite powerful on large scales where it feeds the terminal radio lobes. Conversely, in radio-quiet AGN the outflow is either stopped or loosely collimated in the form of a wind or a bipolar flow. Parallely FR II jets are much more powerful than in FR I with a higher degree of collimation and terminal hot spots. Simultaneously the environment of the jets in FR I sources seems richer than in FR II ones. Various possibilities have been suggested. The radio-loudness could be related to: (i) the host galaxy type [90], (ii) the black hole's spin separating the lower spin radio-quiet galaxies from the higher black hole spin in radio-loud galaxies [6,105], (iii) the differences in the rate of nuclear feeding [81,3], (iv) the different composition of the plasma [25], or (v) the different interaction with the ambient medium [43]. Nevertheless, none of these scenarios seem to be completely satisfactory because for all of them counter-examples may be found. We suggest at the end of this review a quantitative physical criterion for such a transition from radio-quiet to radio-loud galaxies which may, in fact, reconcile those various points of view by taking a different approach.

1.3 Towards a similar unification scheme for μ Quasars ?

The galactic counterparts of the extra-galactic AGN were discovered recently by Mirabel and collaborators ([68] and references therein). Although the central black hole is not supermassive but just of the order of one solar mass, M_{\odot} , they also have relativistic ejecta with similar beaming effects. It is of course too early to draw a precise classification of such objects, since their number is rather small in comparison to AGN. Nevertheless, there seem to exist μ -Seyferts and μ -quasars ([32,38] and Fender's review in this volume for details), with prototypes GX 339-4 and GRS 1915+105, respectively (Fig.

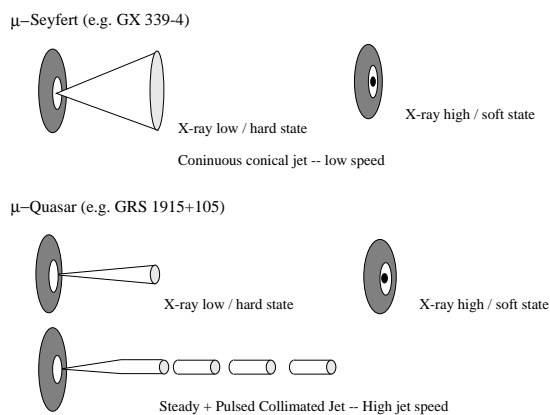


Fig. 3. Summary of the outflow properties of the galactic counterparts of AGN [38]. See text for details.

3). The winds of μ -Seyferts seem to be more continuous and conical while μ -quasars seem to have steady outflows in addition to pulsed collimated jets with higher speed ([35] and references therein). However, these objects show also in X-rays low/hard states where the ejection is present and a high/soft state where no outflow is produced, probably because of the disruption of the disk in the immediate vicinity of the central black hole. It is also interesting to note that especially in GX 339-4, the presence of the wind is associated with an extended X-ray corona at its base.

Note that we do not include in the present discussion all galactic relativistic jets from other binary systems but only those which have similar properties with AGN. Nevertheless, most of the mechanisms reviewed here apply also to such jets as they also apply, incidentally, to jets from young stars, stellar winds, etc. This may explain why the application of the theory of MHD winds, in jets from Young Stars and AGN has evolved parallelly.

1.4 Some key problems about jet formation

The basic questions for understanding the physics and role of jets in AGN and μ -quasars and their complex taxonomy are those related to the nature of the constituting plasma, their initial acceleration in the near environment of the central black hole, their morphology as they propagate away from the central region, the connection of the source (disk, disk corona or black

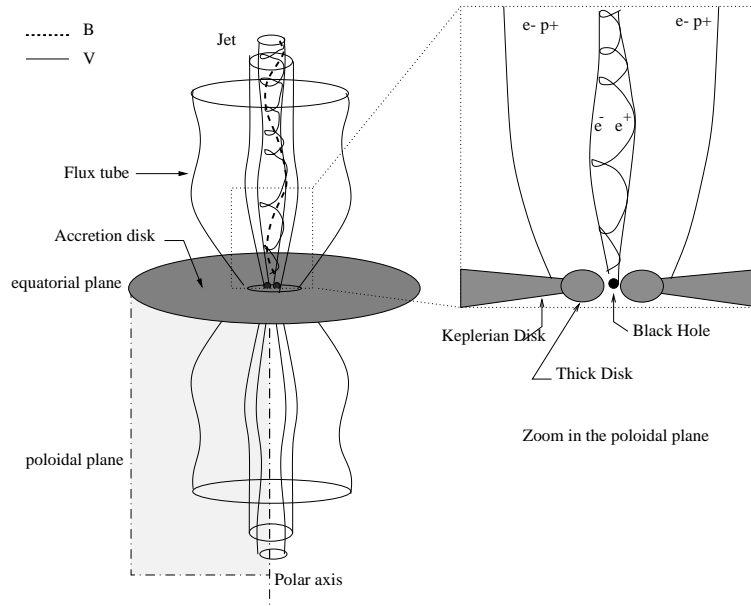


Fig. 4. View of the jet formation region.

hole magnetosphere) and extraction of angular momentum from it. Fig. 4 illustrates how the plasma is extracted from the magnetized rotating source, spiraling and carrying roped magnetic field lines.

Let us briefly recall here some points which we will not address in detail in the remaining part of this review.

First, it is likely that jets associated with quasars are a mixture of electron/proton and electron/positron pairs, since pure electron/positron jets overpredict soft X-ray radiation from quasars, while pure proton- electron jets predict too weak nonthermal X-ray radiation [89]. In fact, it has been suggested first by Sol et al. [88] that jets consist of electron/positron pairs close to their axis, surrounded by an electron/proton plasma (see Fig. 4). This model has known some success since then [78,8] and it may naturally account for the presence of ultra-relativistic flows in the parsec scale made of pair plasma or a mixture of the two while the lobes at larger scales would be fed with the proton-electron part. In this picture the lobes become illuminated by the faster inner jet at some point due, for instance, to an instability that disrupts the jet. It accounts also for the tremendous energetic power observed in the lobes which does not need to be transported directly by the inner pair plasma.

Second, rotating outflows extract also rather efficiently angular momentum from their source allowing thus mass to accrete to the central object. This removal of the angular momentum of the accreted material is very efficient in the presence of the magnetic field, as is happening in stellar magnetic braking [86]. In fact, the magnetic lever arm ϖ_a at the point where corotation ceases is larger by a factor of order 10 than the cylindrical radius of the footpoint of a fieldline, ϖ_o (see Fig. 7b, [92,64]). It is interesting that even if a tiny percentage of order of 1% of the accreted mass rate \dot{M}_{acrr} is lost through a jet, \dot{M}_{jet} , the major part of the angular momentum of the infalling gas is removed and so this gas can be freely accreted by the central object (see [92] for a simple explanation). However, though angular momentum extraction by the wind can be sufficient to account for the accretion (e.g. [40]), turbulent viscosity triggered by some instability can also allow for accretion. In this case, the outflow is likely to exist nonetheless (e.g. [23]). Thus the presence or not of a jet is certainly not an evidence of what really triggers the accretion, though it certainly puts some strong constraint on it.

Let us just clearly state here that in the following sections we will mainly concentrate on the mechanisms which can produce *acceleration*, explain *collimation* and the related *nature* of the source in each case. We refer to various reviews [92,64,9,10] where complementary issues on the problem are treated in more detail. We are not addressing here the question of the propagation of the jet far from the source, its connection to the lobes and the external medium as this is the subject of other reviews in this volume (e.g. Aloy) and other contributions of the conference.

2 Basics of Jet Formation Theory

2.1 The outflow MHD equations

Since the outflows we are describing are made of tenuous electron/proton or electron/positron plasma they can usually be modeled to zeroth order via the set of the ideal MHD equations. Of course the collision rate may be so low that thermalization is not complete and each species should be treated separately. However, even in the well studied case of the solar wind where densities are probably even lower than in relativistic jets the fluid approach has proven to be very efficient and better than a pure collisionless one in describing the dynamics of the outflow. We shall not give here the general axisymmetric equations which can be found in the literature (as, for instance, in this volume). Though it is an observed fact that at least part of the extragalactic outflows are relativistic in velocity or temperature, it has been shown that the basic physical mechanisms at work for the formation of jets are the same with those operating in the classical regime, e.g., [33,47]. Thus, in the following we will not distinguish between relativistic and non relativistic approaches, unless some noticeable difference exists.

The full relativistic set of ideal MHD equations in the 3+1 formalism can be found in [19] for instance and their reduction to the classical Newtonian limit in [17]. They constitute a set of highly nonlinear and coupled partial differential equations of the four spatio-temporal variables. Note that in the following we shall use indifferently spherical (t, r, θ, φ) or cylindrical (t, ϖ, φ, z) coordinates. To describe the flow one needs then to determine its:

- mass density ρ ,
- velocity field \mathbf{V} ,
- magnetic field \mathbf{B} (and electric field \mathbf{E} in a relativistic treatment)
- gas pressure P (or equivalently, the temperature T) of the fluid.

This can be done by combining Maxwell's equations for the electromagnetic fields with the conservation of mass, momentum (Euler's equation) and energy for the hydrodynamic fields. The energy equation is usually (but not always) replaced by the simplifying assumption of a polytropic equation of state.

Under the assumption of steadiness ($\partial/\partial t = 0$) and axisymmetry ($\partial/\partial\varphi = 0$), the toroidal components (B_φ, V_φ) can be expressed in terms of the poloidal quantities [17]. Simultaneously, the magnetic field on the poloidal plane $[r, \theta] \equiv [\varpi, z]$ (Fig. 4) is defined by means of a scalar magnetic flux function A , $\mathbf{B}_p = (\nabla A \times \hat{\varphi})/\varpi$ and the velocity field on the poloidal plane is also defined by means of the mass flux function Ψ , $\mathbf{V}_p = (\nabla \Psi \times \hat{\varphi})/\varpi$. Note that $\Psi = \Psi(A)$ because of the flux freezing law of ideal MHD. Practically, magnetic field lines and flow lines are roped on the same mass/magnetic flux tubes as shown in Fig. 4. Then the momentum equation splits in the

poloidal plane into a component along each poloidal streamline and a component across it. Momentum balance along the poloidal flow (the Bernoulli equation) may be combined with momentum balance across the flow (the transfield or Grad-Shafranov equation) to form a system of two coupled partial differential equations for the density ρ and the magnetic flux function A .

Irrespective of using a polytropic equation of state between pressure and density, or not, this system contains integrals that depend only on the magnetic flux distribution, such as:

- the mass to magnetic flux ratio, $\Psi_A(A) = d\Psi/dA$,
- the total angular momentum, $\bar{L}(A)$,
- the angular velocity or rotational frequency of the footpoints of the magnetic fieldlines anchored in the wind source, star or disk, $\Omega(A)$, which is also the corotation frequency.

Note that $L/\Omega = \varpi_a$ must be the cylindrical radius of the field line A at the Alfvénic transition in order to ensure a smooth Alfvénic transition.

If a polytropic equation of state is used, an extra conserved quantity exists by integrating the momentum equation along the flow: this is the energy per unit mass, $E(A)$, which includes kinetic energy, enthalpy, gravity and Poynting flux. Usually the polytropic index is less than the adiabatic one (and even less than $3/2$) in order to allow for thermal acceleration [76]. This is just a way to circumvent the solution of the rather difficult problem of solving the full MHD equations by selfconsistently treating the heating supply in the plasma. In fact even if no polytropic assumption is made, a generalized form of the energy conservation can be written including a heating and cooling along the flow [84]. Some authors (e.g. [83]) prefer to use the energy in the corotating frame of rotation E' to show in this non Galilean frame explicitly the centrifugal potential. The two notations are equivalent and $E = E' + L\Omega$ where $L\Omega$ (called the “the energy of the magnetic rotator”) is the energy a magnetic fieldline needs to corotate at frequency Ω and plays a crucial role in magnetic acceleration.

The remaining part of this section, despite that equations are not given, is rather more technical and the reader interested in the physical mechanisms at work may well skip it.

2.2 Axisymmetric and time-dependent numerical simulations

The time-dependent MHD problem has been treated only by means of numerical simulations for obvious technical reasons. Thus, there have been performed simulations of relativistic or non relativistic disk winds [75,49,100,101], outflows from a spherical magnetosphere [16,96,51,99] or, from both types of sources [52,55,70,56]. However, in some simulations it is not clear that the boundaries do not introduce spurious effects (e.g. [75,49]) or, that the system

relaxes into a reproducible final state (e.g. [52,55,70,56]). Another difficulty with the numerical simulations has to do with the fact that AGN jets often extend over lengths more than six orders of magnitude their width, while the available grid sizes are much smaller. One way out of this constraint is to solve the problem via a combination of numerical techniques for the near zone and analytically solving the hyperbolic steady state problem at large distances from the central source (e.g. [16,96], although the very first accelerating region close to the base is not treated).

2.3 Axisymmetric and steady analytical solutions

Several solutions of the steady MHD equations for various sets of boundary conditions are available analytically while there exists only one numerical solution for a specific and quite unique set of boundary conditions obtained by Sakurai [83] for stellar winds showing very weak collimation (i.e. logarithmically) around the rotational axis. Basically the main difficulty is the fact that the set of the steady and axisymmetric MHD equations are of mixed elliptic/hyperbolic type, as opposed to the hyperbolic by nature time-dependent equations. Then, from the causality principle, a physically acceptable solution needs to cross three critical surfaces: the slow magnetosonic, the Alfvénic and the fast magnetosonic surfaces. However, the exact positioning of those critical surfaces is not known *a priori* but is only determined simultaneously with the solution. It is for this reason that only a few classes of such exact MHD solutions have been studied so far. They can be obtained by employing a separation of the variables (r, θ) in the poloidal plane (see Vlahakis and Tsinganos [103] for a general technique to obtain such solutions) combined with a suitable choice of the MHD integrals Ψ_A , $L(A)$, $\Omega(A)$ and $E(A)$. It is worth to note that this systematic construction unifies all existing analytical models of cosmic outflows, such as the classical Parker wind [76] and the Blandford and Payne disk wind [11], in addition to uncovering new and interesting global models [103]. The best studied classes of such solutions are characterized by radial and meridional self-similar symmetries because all quantities scale with the spherical radius r or the colatitude θ respectively.

The *first* family with radially self-similar symmetry is appropriate to winds emerging from disks (e.g. [2,11,31,63,57,24,104,103] and references therein). A relativistic extension of these self-similar models exists (see e.g. [61]) although by dropping one essential element: gravity. No intrinsic scale length exists in this case and all quantities scale as a power law of the radius, similarly to the Keplerian law for the velocity in the disk. The key assumptions in this class of solutions are that the poloidal Alfvén Mach number M and the cylindrical radius ϖ of a particular poloidal fieldline $A=const.$, in units of the cylindrical radius ϖ_a at the Alfvén point along the same poloidal fieldline, are solely functions of the colatitude θ . In this case surfaces of constant M are assumed to be conical, and the critical surfaces too.

The *second* family is characterized by the meridional self-similar symmetry and is appropriate to winds emerging from a spherical source, although the physical variables are not spherically symmetric and the boundary conditions are functions also of the colatitude ([94,85,103] and references therein). Even though these solutions seem to be more natural to describe stellar winds, they do not exclude the presence of a surrounding accretion disk and they can on an equal footing describe a quasi spherical corona or magnetosphere around the central object. The key assumptions also in this case are that the poloidal Alfvén Mach number M and the cylindrical radius ϖ of a particular poloidal fieldline $A=const.$ are solely functions of the spherical radius r . In this case surfaces of constant M are assumed to be spherical and so are the critical surfaces.

2.4 Boundary conditions and singularities

As we mentioned in the previous section, for the construction of a steady solution one has to carefully cross the appropriate critical surfaces encountered at the characteristic MHD speeds, corresponding to the three MHD waves propagating in the medium (but not to the elliptic/hyperbolic transitions as we discuss in the following). It effectively results in reducing the number of free boundary conditions [15]. Note that in the relativistic case the number of critical surfaces is the same with the nonrelativistic case because the light cylinder singularity is combined with the Alfvénic one [17]. As a corollary, this generalized Alfvénic singularity reduces to the classical one in the non relativistic regime and to the light cylinder when the mass loading is negligible.

It is conventional to associate the crossing of the slow surface to fixing the mass loss rate and the crossing of the Alfvén to fixing the magnetic torque

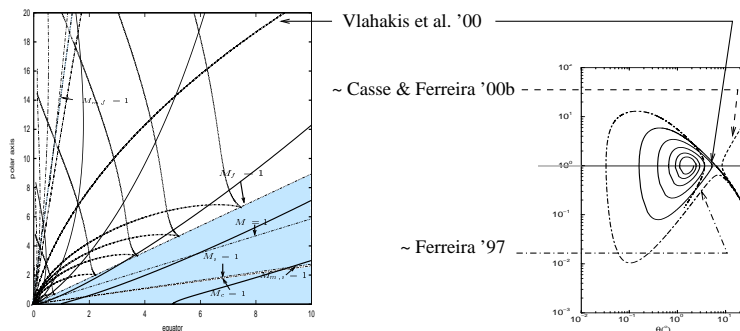


Fig. 5. Topology of an analytical disk wind solution in the region of the fast magnetosonic transition in the $[M_f, \theta]$ plane. Examples of three solutions of this type are drawn: one that crosses the critical point and two which do not.

[92]. The crossing of the last singularity usually remains more subtle but is essential to ensure that no instability or shock with the external medium is going to propagate backward and possibly changes the structure of the solution. This is well known for the Parker solar wind, where terminal shocks will naturally make breeze solutions to evolve into the wind solution.

To illustrate this point we show in Fig. 5 three disk wind solutions belonging to the radial self-similar class and the topology of another typical set of such solutions around the fast surface in the plane of colatitude and fast magnetosonic Mach number (instead of the Mach number for a classical hydrodynamic wind). A careful look at the behaviour of those solutions shows that one is crossing exactly the fast magnetosonic transition [104] while the other two behave close to the critical surface either like a breeze solution [40] or like a terminated solution [24] in Parker’s terminology for the solar wind, as illustrated on Fig. 5. Although they differ in the way they connect to the underlying disk, they basically show very similar properties. This indicates that, by tuning the heating deposition along the flow or the polytropic index, a physical connection with the disk and the crossing of the fast point is possible despite it has not been done yet. It also suggests that the crossing of the last surface is not so crucial for the connection with the disk but it validates, nonetheless, the widespread use of such disk wind solutions. In fact all solutions terminate after some point due to the presence of a spiral singularity as shown in Fig. 5, which makes even more crucial the presence of a shock not only from observational arguments but also from theoretical ones.

2.5 Singularities and horizons

We discuss now the true nature of the singularities, pointing out that a strict analogy between MHD signal propagation and the light propagation in the neighborhood of black holes (see Carter [22]) exists.

First, as it is well known in the theory of steady and spherically symmetric black holes (Schwarzschild black holes in the case of vacuum), the horizon where no information or light signal can escape coincides with the ergosphere where the system of the relativistic equations changes nature, from elliptic outside the horizon to hyperbolic inside it. As illustrated in Fig. 6a the system is hyperbolic in time and information emitted at the speed of light propagates along a “cone”, the light-cone. In a steady state and far from the black hole, the light-cone’s projection is a circle and thus information can propagate in all directions of the $X_1 - X_2$ plane, similarly to water waves on a static pool. X_1 and X_2 are two coordinates in space. The equations are elliptic. But because of gravity, light is deflected and inside the horizon, equations change to hyperbolic, the cone projection gives characteristics, as the trail of a boat, and information can propagate only inside these. Furthermore, all characteristics converge to the center of the black hole such that no information can escape (Fig. 6a).

The same is true and well known in MHD outflows where light is replaced by MHD waves and the spatial coordinates are reversed (X_1 corresponding to $1/X_1$) such that the center of the black hole becomes the asymptotic outer connection of the MHD outflow with the extragalactic medium. In spherically symmetric outflows (or equivalently when the poloidal geometry of the flow is fixed), each of the three singularities coincides in fact with a spherical surface which marks the transition in the nature of the equations from hyperbolic to elliptic¹.

Second, if the black hole is rotating, the event horizon and the ergosphere where the system changes from elliptic to hyperbolic split. It is easy to understand this physically (see Fig. 6b). As the geodesics rotate, the light cone first inclines itself such that beyond the ergosphere characteristics appears. One of the family of characteristics still connects with the external medium so it is still possible to propagate information backward. Once inside the real horizon the light cone is inclined and directed towards the center. At this point the outer space is causally disconnected from the interior of the horizon.

¹ There is an extra transition at the cusp velocity which is not a singularity while the Alfvén singularity is in a parabolic domain but we shall not enter here in these details.

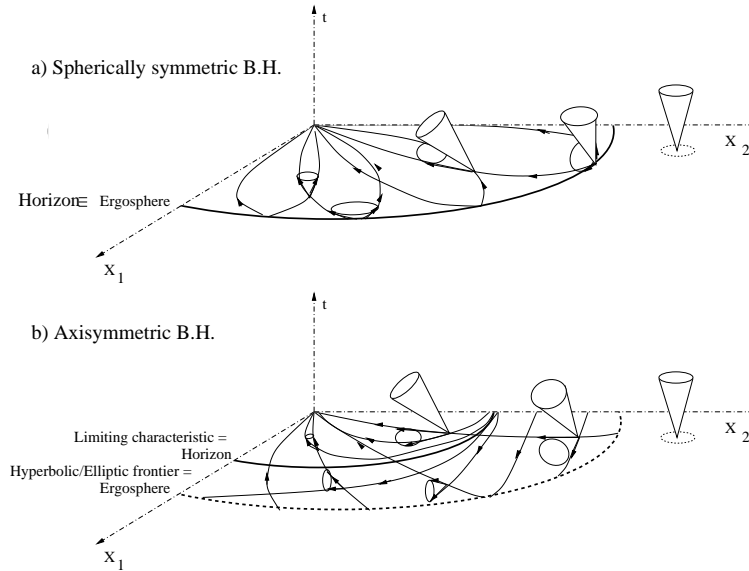


Fig. 6. Ergosphere, horizon and light cones around a black hole after Carter [22]. Time is along the vertical axis and space in the horizontal plane [X_1, X_2]. In a) sketch of a spherically symmetric black hole and in b) a rotating axisymmetric one.

The analogy between the event horizon and the MHD singularities in terms of limiting characteristics or separatrices has been recently recognized [15] and illustrated explicitly by examples of self-similar solutions [95]. Note that for the slow magnetosonic horizon the situation is a bit more complicated because the slow waves have triangular wave fronts instead of circular [102]. However, the ultimate horizon is the one associated with the fast waves. In addition, the so-called “classical” critical points correspond to the ergosphere where the equations change from elliptic to hyperbolic. This point has been underestimated. In fact, it is known for the ergosphere of black holes that it can appear as a singularity but a suitable choice of the Killing vectors eliminates it. The same must be true for the “classical” critical points where the poloidal velocity equals one of the wave speeds.

Third, the analogy can still be pushed one step further. There are only two cases where the horizons can be defined locally, either, for static black holes where the horizon coincides with the ergosphere (Fig. 6a), which corresponds to the spherical Schwarzschild solution in vacuum, or, in the circularity limit where the horizon coincides with the rotosurface, which means that there is only rotation and no convection. In all the other cases, the horizon can be defined only globally that is as a limit of the characteristics, once the solution of the metrics is known (i.e. as a limiting characteristic).

The circularity limit for the vacuum solution corresponds to the Kerr rotating black hole (Fig. 6b). In this special case, one can construct the solution [22], by means of a separation of the variables r and θ while t and φ are ignorable. The θ component can be solved by using Legendre’s polynomials. This way of constructing the global solution is identical to the one used for self-similar flows. In both cases the form of the singular surfaces is known a priori and this is definitely NOT the self-similar assumption that “modify” the critical points as we have written for so long.

The first conclusion is that in the more general axisymmetric case, there is little hope that we can determine the limiting characteristics *a priori* in MHD outflows. However, these are the true singularities of the flow.

The second conclusion is that this problem of horizons concerns not only steady solutions but also numerical time-dependent solutions. Even if they do not appear as real mathematical singularities, they must be present in the sense that characteristics on the outer boundaries should all be directed outwards, which has not been the case of all simulations as we already mentioned.

3 Acceleration

Once valid solutions of the outflow equations are obtained, either numerically or analytically, we may study the physical mechanisms that accelerate and collimate the outflow transforming it from a wind to a jet. From a rather general perspective, an observational characteristic of many cosmic plasma

outflows is that they seem to be *accelerated* to relatively high speeds which may even reach values close to the speed of light in the most powerful AGN jets. The most often invoked mechanisms to accelerate these flows are of thermal, or, of magnetocentrifugal origin. We shall discuss first in the following magnetocentrifugal acceleration since it is widely considered as the most relevant mechanism for the acceleration of AGN jets.

3.1 Toroidal magnetic field acceleration

The simplest magnetic driving mechanism is the so-called 'uncoiling spring' model (Uchida and Shibata 1985, [97,56]) or 'plasma gun' [30] where a toroidal magnetic pressure builds up due to the rotation of the fieldlines which are anchored in the disk. Evidently, there is a net force pushing the plasma upwards, as shown in Fig. 7a. This mechanism is mainly seen in numerical simulations (e.g., [87]). After the initial transient phase when a torsional Alfvén wave develops and drives the initial acceleration of the flow, the solutions converge to a weakly collimated structure, where the confinement is done by the toroidal magnetic field. However, for the numerical constraints we mentioned above, the outflow cannot be simulated in regions far from the base to follow realistically its degree of collimation. Second, such numerical simulations were able to follow the jet for one or two rotations around the central body. Hence, such a mechanism seems to be at work only to explain intermittent ejection, something equivalent to Coronal Mass Ejections (CMEs) in the solar wind that travel on top of a global more steady structure.

It is interesting that instabilities by a spiral wave in the disk producing an Alfvén wave have been also advocated to explain the intermittent ejection from μ Quasars[93]. These instabilities can be at work to explain various features, as we briefly shall discuss later and transients on a time scale of a

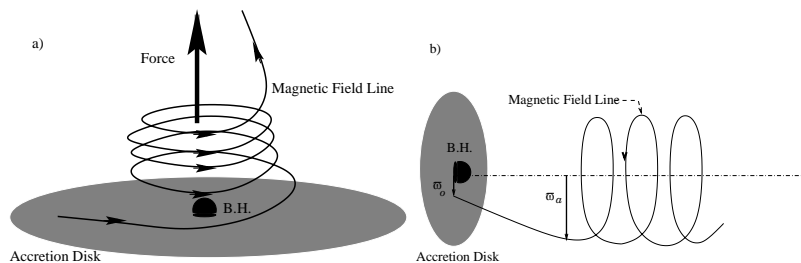


Fig. 7. **a)** Acceleration by toroidal (azimuthal) magnetic pressure. The fieldline is wound by rotation and acts as an uncoiling spring. **b)** Magnetocentrifugally driven wind. The acceleration is similar to that of a 'bead on a wire' and it operates from the disk footpoint ϖ_o up to the magnetic lever arm ϖ_a where corotation stops. Further downstream the magnetic field is rapidly wound up and magnetic collimation is obtained because of the pinching magnetic tension (after Spruit [92]).

few rotations around the black hole. However, we need to model at the same time some more continuous ejection, similarly to the solar wind where despite instabilities and CMEs, there always exists a steady wind outflow.

3.2 Magneto-centrifugal acceleration from the disk

In order to accelerate jets magnetically, the most popular scenario is the magnetocentrifugal acceleration from an accretion disk via the classical Blandford & Payne [11] acceleration mechanism. In this case, the plasma consists probably mostly of electrons/protons, either relativistic or not. Electrons/positrons could be accelerated in the same way but it seems more difficult to produce them above the keplerian disk than in or close to the black hole's magnetosphere for energetic reasons, e.g. [46]. As the poloidal magnetic field is dominant up to the Alfvén radius, it practically enforces an approximate plasma corotation similarly to a 'bead on a rotating wire' (see Fig. 7b). In the corotating frame there is then a centrifugal potential which accelerates the flow outwards provided that the line is sufficiently inclined ($\theta > 30^\circ$ from the pole for a cold non relativistic plasma). Note that this condition is less restrictive if there is some heating or the gas is relativistic [91,92]. This point should not confuse the reader, because the centrifugal force does not alone accelerate the flow but the opposite and it is its combination with a strong poloidal \mathbf{B} field that allows for the acceleration. Eventually the acceleration comes from the conversion of Poynting energy flux to kinetic energy flux. The gain in kinetic energy is proportional to the energy that brings the magnetic field lines into rotation, i.e., the energy of the magnetic rotator $L\Omega$. Such a magnetocentrifugal driving mechanism seems to be efficient in disk winds wherein a hot corona is not an absolute requirement.

Besides a long list of self-similar models (see [103,53,54,74]), the same mechanism has shown to be successful in various numerical simulations [75,49].

This mechanism has some limitations. For example, it requires high magnetic field strengths at the disk level (which have not been measured so far) and also a large magnetic lever arm is needed in order to obtain a terminal speed which is a few times the Keplerian speed ($\lesssim 10^5$ km/s). Moreover, only a very small fraction of the accreted mass can be ejected at very high speeds, once a connection with a realistic disk structure is properly made [40,63,23]. By realistic disk structure we mean that in the accretion disk resistivity, turbulence and viscosity are taken into account within the hypothesis that the disk is pervaded by a large scale mean magnetic field. However, the presence of a hot corona on top of the disk is enough to eliminate this limitation [24]. If these conclusions hold unchanged in the presence of a local dynamo and/or disordered magnetic field is not clear yet [45,10].

3.3 Magneto-centrifugal acceleration from the black hole magnetosphere

A wind outflow could also be extracted “magneto-centrifugally” from a black hole’s magnetosphere through the Blandford & Znajek mechanism [13] (see also [10] for more references). First, the rotational energy of the accreting black hole is extracted by a large scale magnetic field accreted onto the black hole, then converted to Poynting flux and finally to relativistic electron/positron pairs. As far as the plasma itself is concerned there is no difference with the previous mechanism, since it is ultimately the Poynting flux that accelerates it. However, there are two basic differences. First, the Poynting flux is extracted from the black hole. This is physically consistent since some angular momentum of the opposite sign is lost simultaneously into the black hole. Second, there is enough energy in the magnetosphere to produce electrons/positron pairs, such that this mechanism favors leptonic ejection. It has been argued that pairs would suffer Compton drag; however, this may be a real problem for radiatively driven winds but not if there is an extra mechanism to accelerate the flow sufficiently to overcome these radiative losses.

The efficiency of this mechanism has been recently put into question by several authors (see for instance [65]). The main argument is that the extraction of energy from the black hole through this process is at most as efficient as the extraction of energy from the disk. This only means that the two mechanisms are likely to operate simultaneously. Again this could very well be in favour of a leptonic jet or beam extracted from the black hole embedded in a hadronic heavy wind/jet coming from the disk [88,46]. Moreover this does not apply necessarily to the gamma ray emission which may still get its energy from the black hole [10].

3.4 Radiative acceleration

The first alternative to a magnetically driven wind is a radiatively driven wind. For instance, in the ‘Compton rocket’ model a disk produces electron/positron pairs which are accelerated by the radiation produced by the annihilation of this plasma. Although Compton radiative losses exist they are not sufficient to prevent completely the plasma acceleration [71,27].

Radiatively driven models for disk winds of electrons/protons have been proposed with a radiative pressure due to dust or, due to lines coming either from the disk or the central source (see [79] and further references in the introduction). The key point in such models is that they result in at most a few tens of thousands of km/s for the outflow speed ($\sim 50,000$ km/s). This may be enough to explain most of the winds from radio quiet AGN, but it is unable to explain the acceleration of the powerful jets associated with radio loud AGN, or, the mildly relativistic flows seen in some radio quiet AGN. It is thus likely that in those objects, radiative acceleration may

operate as a minor contribution or, in combination with other mechanisms, like magnetocentrifugal driving [53].

Alternatively, it has been shown that a magnetized cloud of relativistic electrons can be radiatively driven up to relativistic velocities if the interaction between photons and particles comes through a synchrotron process [41,42]. However the cross section of this mechanism is critically dependent on the geometry of the interaction and some assumptions are necessary ‘a priori’ for the treatment of the equations.

3.5 “Thermal” acceleration

The other alternative to magnetic acceleration is classical thermal driving, as it is the case in the low- and high-speed solar wind where the heating and part of the pressure is provided by the dissipation of acoustic waves, electric currents, etc., or more efficiently by Alfvén waves. In this case the presence of a hot corona around the disk and/or the magnetosphere is essential for the acceleration, which is proportional to the sound speed, i.e., to the square root of the coronal temperature.

Then, in a rather crude estimate, if the 10^6 K corona produces a thermally driven wind with a terminal speed around 300 km/s, a corona with a temperature of 10^9 K for both the ions and the electrons could result in a terminal speed around 10,000 km/s. On the other hand, if 10^9 K is the temperature of the electrons while the temperature of the protons is 10^{12} K, a wind results with a terminal speed of the order of the speed of light, 300,000 km/s. Of course at this point relativistic effects should be taken into account properly. For ultra-relativistic flows the adiabatic sound speed is only $c/\sqrt{3}$; however, this is without taking into account the existence of extended heating in the corona. Most of all the heating by waves, in particular (torsional) Alfvén waves, could be very efficient. For instance, it has proven to be efficient enough, even with small amplitudes, to explain the 800 km/s of the fast solar wind [99]. By extrapolation, we may guess that it should be able to produce very high speeds in AGN outflows. Waves of large amplitudes could be even more efficient, producing turbulence, and this is not very different from the transient torsional Alfvén “wave” seen in numerical simulations [56], except that the production of such waves should be continuous.

In fact, this mechanism combined with magnetocentrifugal driving, has found some success in the literature [64], like for the acceleration in the corona from ADIOS [7], from a Keplerian disk [24], from a black hole magnetosphere through a shock [34,52,55] or, more in general, from any kind of spherical corona [84,94,85].

Thus, thermal acceleration in a broad sense is likely to be as efficient as the magnetic processes. We could then suggest that both may be at work in disk winds for electron/proton plasmas (where it also allows to have higher mass loss rates, as we already mentioned [24]) while the electron/positron pairs would be more likely magnetically driven from a black hole magnetosphere.

This seems also to be suggested by recent numerical simulations [52,55] in which two flow streams are accelerated near the black hole after passing through some shock in the accretion disk. Despite the fact that the disk is governed by ideal MHD and it is not clear if the simulations can hold more than one or two rotation times, it is worth to note that these simulations show a double component of the wind, a inner magnetocentrifugally driven part and an external pressure driven component.

4 Collimation

Once the outflows are accelerated, they will propagate in the form of either collimated beams or uncollimated winds. However, apart for the case of the solar wind, uncollimated flows are hardly observable, while jets are observed in several astrophysical environments, from star formation regions to distant AGN. This is mainly due to the much higher density inside jets as opposed to that in loosely collimated winds. Furthermore, in radio-loud AGN where beams move at relativistic speeds, the emission may be largely amplified by Doppler boosting if the jet is pointed towards the observer, which is probably not the case in radio-quiet sources. Again the two basic mechanisms responsible for collimation may be of thermal or magnetic origin.

4.1 Pressure confinement

An outflow is thermally confined if the surrounding medium has a higher pressure than the flow, such that there is a pressure gradient forcing the outflow to collimate along its ejection axis. In other words, only outflows underpressured with respect to their surrounding environment may be thermally confined. In fact, such a situation seems to occur in many extragalactic jets, as deduced from X-ray data implying a hot plasma surrounding early-type galaxies and clusters of galaxies [39].

The 'twin exhaust model' based on an analogy with the De Laval Nozzle, was the first effort to thermally confine jets [12]. However, this confining mechanism has been by now excluded because it requires the throat of the nozzle to be located rather far from the central object, as it works for both collimating and accelerating the flow. To remedy that, the idea of an external medium but only collimating the outflow has been suggested [36]. Meridionally self similar models [94,85] have shown that cylindrical collimation could arise naturally from inward pressure forces but with some contribution by the magnetic field too. In an pure thermally collimated flow at the end the jet should collapse onto the rotational axis, unless it rotates fast enough such that the centrifugal force may counteract the external pressure. However, the strength of rotation is likely to be related to the strength of the magnetic field (because of dynamo for instance) such that they are usually low simultaneously.

So thermal confinement may play a role in FR I and Seyfert types of AGN but probably not in FR II which are known to have a very poor environment so there cannot definitely be a unique mechanism for all AGN.

4.2 Poloidal magnetic confinement and subfast flows

With toroidal magnetic fields known to be unstable in tokamaks, it has been suggested that toroidal confinement and pinching should be unstable, and collimation could be achieved by poloidal magnetic fields alone [91]. This is supported by the parallel magnetic field measured at small parsec scales in some extragalactic jets [92]. However recent observations of highly optically-polarized compact radio-loud quasars (HPQ) has shown that the electric vectors of the polarized 43 GHz radio cores are roughly aligned with the inner jet direction indicating magnetic fields perpendicular to the flow [66]. Magnetic fields are also known on larger scales to be perpendicular to the jet axis in FR II sources while they are parallel to the jet axis in many FR I sources. However parallel does not necessarily mean that it is not helicoidal and there is no toroidal field. The parallelism could simply be due to a strong velocity shear across the jet's cross section as it is explained in [10].

Poloidal magnetic fields can induce some mild collimation in the outflow in the region from the disk up to the Alfvén transition (see Fig. 7b) where the plasma in the transfield equation governing the morphology of the flow is basically dominated by magnetic forces. Beyond this distance, the jet becomes superAlfvénic and the hydrodynamics of the flow overcomes magnetic forces, in such a way that collimation will stop. To continue poloidal collimation on large distances, the jet must remain subalfvénic. But then, the jet will be very sensitive to shocks and instabilities that can propagate upstream from far distances and destroy the whole equilibrium.

Similar problems occur in asymptotically cylindrical solutions [31,74] of radially self-similar disk-wind models. Subfast outflows as those proposed by Ostriker [74] attain only low Alfvén Mach numbers and such solutions are structurally unstable [104]. In fact, as we already wrote, all the other solutions of those models are terminated because of the spiral singularity (see Sec. 2.4).

4.3 Toroidal magnetic confinement and stability

Another confining mechanism, which is in fact supported by observations [66], is the magnetic confinement of the outflow by a toroidal magnetic field wound around the jet, the so-called hoop-stress paradigm [92]. This mechanism works both for under- and over-pressured jets. Observations of perpendicular magnetic fields [66] imply that such beams carry some electric current that eventually closes at their surface or outside. Note that the building of the toroidal magnetic field is done at the expense of the Poynting flux. Thus, in a pure magnetic jet all the Poynting flux cannot be converted to kinetic energy, if part of it remains to confine the jet. Obviously reality in most cases,

and particularly in the case of AGN, may involve a combination of thermal and magnetic processes in the acceleration and confinement of the outflow.

Despite the observations that we mention above, there is still a vigorous debate on whether magnetic instabilities may ultimately disrupt the jet, or not. In particular, it has been shown in the context of a pure magnetic jet without rotation that instabilities are always present [4]. Rotation in a pure hydrodynamic flow is also known to have a destabilizing nature and hydrodynamic instabilities may also disrupt the jet [14], though relativistic jets are more stable (see Aloy this volume). However, the combination of toroidal magnetic fields and rotation is more subtle, since the two ingredients act in opposite directions.

Recent numerical simulations and extended analytical work [48] gave support to the result that magneto-rotational instabilities may develop rapidly. Such instabilities for a cold plasma tend to favor the formation of an inner denser core in a jet. Similar results have been obtained from a local analysis of the ballooning modes [50], though there is no precise calculation of any growth rate. In particular, the inner part of the jet with a vanishing current density on the polar axis, is particularly unstable to magnetic shearing in this analysis.

On the other hand, a non linear analysis of current driven instabilities ([59] and ref. therein) has shown that the instability instead of disrupting the jet leads to a reorganisation of the current density. Instabilities in more complex jets from Keplerian disks have also been studied [60] and present interesting structures, again forming a dense core jet surrounded by a return current in a cocoon.

Parallely, magnetorotational instabilities have also been studied using the flux tube approximation [44], which is likely to give the most unstable mode, including only toroidal fields but with all the other ingredients, such as shearing or buoyancy. This study agrees with the fact that jets with a Keplerian velocity profile, as well as the outer region where the jet connects to the external medium are subject to strong instabilities. Conversely, the inner parts of a jet can be completely stabilized for a flat, or a solid rotation profile, provided – and this does not appear in the studies mentioned above – that there is an increase of the density away from the axis. In this case jets from the central source, like those obtained in meridional self similar models, should be more stable than jets from Keplerian disks. It also explains the edge brightening seen in some sources, because the instabilities are likely to occur mostly at the edges. Eventually instabilities are sources of reacceleration in the plasma and ultimately radiation. Finally, it suggests that hollow jets (not empty jets!) should be more stable than dense core ones.

Altogether, then it follows from both, observations and theoretical studies, that one better be careful before claiming that toroidal instabilities will disrupt rotating MHD jets. However, instabilities do in general exist and they are obviously a crucial element for explaining a few structures we see in both

observed jets and simulations. The issue is rather crucial and is a subject by itself in this volume (see the article by Aloy).

4.4 Asymptotic equilibria

With hoop stress and pressure gradients collimating winds into jets, it is interesting to wonder which kind of asymptotics the outflow takes. A useful general analysis for magnetically dominated flows has been performed by Heyvaerts & Norman [47], generalized to relativistic flows in [33].

In the case where pressure and centrifugal forces drop asymptotically faster than the magnetic forces do, then the final equilibrium state should be force-free, and the asymptotical morphology of the flow is related to the electric current flowing. To summarize, a given flux tube collimates to

- *cylindrical* asymptotics if there is a net poloidal current spread in it;
- *paraboloidal* asymptotics if the net poloidal current is zero;
- *radial* asymptotics if there is a net current but it flows inside the region of the radial asymptots.

Of course, the whole jet could be in principle cylindrical if the return current lies outside the jet or, in a current sheet (cf. observations [66]). Note that flows with return current sheets are known to exist and the best example where it is observed and measured *in situ* is the solar wind. However from the analysis of Heyvaerts & Norman (1989) the possibility of mixed asymptotics with cylinders surrounded by cones (=radial asymptotics) is not excluded. Asymptotic solutions of such flows have been successfully constructed especially in the context of relativistic flows either for pure cylindrical asymptots [37]) or mixed radial and cylindrical (e.g. [69],[16]).

An analogous analysis to [47] has been recently proposed, which nevertheless arrives to opposite conclusions [72]. It extends the study to the quasi-asymptotic domain (called asymptotics), i.e. for $z \lesssim \infty$ and connects the curvature of the streamlines to the direction of the current density. It is shown that the collimating part of the outflow is related to the enclosed current, while the outside region of return current should cause the outflow to decollimate. However, it is postulated that cylindrical and radial asymptotics are not accepted as a valid possibility in MHD outflows because of their “violation of causality” and because cylinders correspond to a specific direction, as claimed therein. Instead, a continuous deflection towards the polar axis or the equatorial plane is preferred. However, this inevitably leads to an inconsistently infinite density there while close to the polar axis the underlying assumptions are not valid any longer as we explain below. A more interesting relativistic generalisation of these results is obtained in [5] where collimation is not rejected as a possibility but it is pointed out that the presence of decollimated flows could explain strong equatorial flows seen around several compact objects.

All previous results rely on the strong hypotheses that pressure and centrifugal forces drop asymptotically. In order to have this, two assumptions are made. First, that the cylindrical radius of any flux tube is assumed to be much larger than its value at the Alfvénic transition $\varpi/\varpi_a \rightarrow \infty$ – this is not necessarily true for cylindrical asymptots even for $\varpi \gg \varpi_a$. Second, it is assumed that we do not remain too close to the polar axis [72]. More general asymptotics have been found [84,94,85] including pressure and rotation but using the assumption of meridional self-similarity which cannot hold indefinitely far from the axis (where the return current is well known to exist for instance). Cylindrical and radial asymptots are found in agreement with the Heyvaerts & Norman [47] conclusions despite the different assumptions.

Then, after considering the asymptotic behaviour in general, one needs to connect it to the source [37,58] and if possible by solving selfconsistently the transfield equation [84,94,103,85,16,96], a topic we take up in the next section.

5 On a possible classification of AGN

5.1 An energetic criterion for the collimation of outflows

Apparently a missing parameter in the vertical classification of AGN in Fig. 2 corresponds to a variation in the degree of collimation, going from the winds of Seyferts, to the jets from FR I and then to the powerful jets from FR II type of AGN. Thus we need a criterion for collimation to get a quantitative information on how much the flow will expand.

In fact several models have found a ‘fastness parameter’ α given by

$$\alpha^2 = \frac{L\Omega}{V_a^2}, \quad (1)$$

where $L\Omega$ is again the energy of the magnetic rotator and V_a the poloidal Alfvén velocity at the Alfvén transition where $\varpi = \varpi_a$. This parameter was originally introduced by Michel [67] to measure the fastness of the magnetic rotator which accelerates the flow of a cold plasma. In an equatorial wind, when this energy dominates we have a fast magnetic rotator and the wind is magneto-centrifugally driven. Conversely, when thermal acceleration is dominant the magnetic rotator is termed slow. It appeared that α also controls the degree of collimation in several analytical models (e.g. Ferreira [40], Léry et al. [58]). In the numerical approach followed by Bogovalov & Tsinganos [16,96] the degree of collimation is determined by a similar parameter α expressing the ratio of the angular velocity times the Alfvén spherical distance to the initial constant speed of an initially nonrotating split-monopole type of a magnetosphere.

In fact in most of these models boundary conditions were exactly spherically symmetric on the source except for rotation [58,16] or, the magnetocentrifugal forces were dominant in collimating and accelerating the flow [40].

If gas pressure gets important and/or the boundary conditions in density are not spherically symmetric, there seems to be some changes in the degree of collimation, although the role of the fastness parameter remains qualitatively the same [96,24]. In the meridionally self-similar approach followed by Tsinganos et al. [84,94,103,85] the degree of collimation is not only related to the fastness parameter but also to the distribution of the thermal content. In particular, specific criteria for the collimation of winds were derived in the frame of these models [84,85] that we shall summarize here.

Usually in an outflow the thermal input in the form of internal energy and external heating is not all fully converted into other energy forms: unless the terminal temperature is zero, there remains some asymptotic thermal content, $h(\infty, A)$. By subtracting from the total energy $E(A)$ the heat content at infinity, $h(\infty, A)$, we obtain a new streamline constant, $\tilde{E}(A)$, which will be the total convertable specific energy along the given streamline A , i.e., the energy which can be converted to other forms. Finally, the volumetric total convertable energy is $\rho(r, A)\tilde{E}(A)$.

It turns out that in meridionally self-similar flows the difference of the volumetric convertable energy between a nonpolar streamline and a polar streamline normalized to the volumetric energy of the magnetic rotator $\rho(r, A)L(A)\Omega(A)$ is a constant ϵ' [85],

$$\epsilon' = \frac{\rho(r, A)\tilde{E}(A) - \rho(r, \text{pole})\tilde{E}(\text{pole})}{\rho(r, A)L(A)\Omega(A)}. \quad (2)$$

This quantity ϵ' plays a crucial role in the asymptotic shape of the streamlines, in the sense that the necessary condition for cylindrical asymptotics is $\epsilon' > 0$. In other words, cylindrical collimation is controlled by a single parameter, ϵ' , representing the variation between a fieldline A and the pole, of the sum of the (volumetric) poloidal and toroidal kinetic energies, the Poynting flux, the gravitational potential and the converted thermal content.

If everything is homogeneous in the medium except rotation and the energy of the magnetic rotator, which always increases away from the axis, then this parameter is very similar to the fastness parameter ($\epsilon' \sim \alpha^2$). Conversely, if the density increases also substantially away from the axis while temperature drops so much that the thermal heating cannot lift the plasma, acceleration will be done at the expense of the Poynting flux. Thus the Poynting flux won't be any longer available to collimate the flow and the degree of collimation will decrease.

In the specific model we are describing, this can be put in a more quantitative form because this parameter splits into two terms [85]:

$$\epsilon' \equiv \mu + \epsilon. \quad (3)$$

μ represents the variation across the streamlines of the thermal content that is finally converted into kinetic energy and gives a measure of the thermal

pressure efficiency to collimate the outflow. ϵ is the efficiency of the magnetic rotator to collimate.

In fact μ can be written

$$\mu = \frac{P(r, A) - P(r, \text{pole})}{P(r, \text{pole})} \frac{V_\infty^2}{V_*^2}, \quad (4)$$

where V_∞ and V_* are the polar asymptotic and Alfvén speeds, and $P(r, A)$ the pressure along the streamline A . For under-pressured flows ($\mu > 0$) the pressure gradient force is outwards helping collimation. Conversely, over-pressured jets ($\mu < 0$) and iso-pressured jets ($\mu = 0$) can collimate only magnetically.

On the other hand, the parameter ϵ is equal to the excess of the magnetorotational energy on a nonpolar streamline which is not used to drive the flow, in units of the energy of the magnetic rotator. It can be evaluated at the base of the flow r_o ,

$$\epsilon = \frac{L\Omega - E_{R,o} + \Delta E_G^*}{E_{MR}}. \quad (5)$$

with

$$\Delta E_G^* = -\frac{\mathcal{G}\mathcal{M}}{r_o} \left[1 - \frac{T_o(\alpha)}{T_o(\text{pole})} \right], \quad (6)$$

where \mathcal{G} is the gravitational constant, \mathcal{M} the central mass and T_o the temperature at the base of the flow r_o . The energy of the magnetic rotator ΩL is mainly stored in the form of Poynting flux, i.e. $E_{R,o}$ (the rotational energy) is usually a negligible quantity in the above expression. In other words, ϵ measures how much of the energy of the magnetic rotator is not used to escape the gravitational well and is available for magnetic collimation alone. If there is an excess of this energy on non polar streamlines, magnetic forces can collimate the wind into a jet. Thus, when $\epsilon > 0$ we have an *Efficient Magnetic Rotator (EMR)* to magnetically collimate the outflow into a jet, and an *Inefficient Magnetic Rotator (IMR)* if $\epsilon \leq 0$ [85].

Results are summarized in Fig. 8 in the parameter space with typical solutions represented in the poloidal plane. For each solution, the lines are simply a cut in this plane of the magnetic flux tubes, i.e. a projection in this plane of the wounded streamlines as in Fig. 4. First we see that jets from EMR are very well collimated independently of being under- or over-pressured, as illustrated with the solution in Fig. 8a. For IMR the situation is more complex. If the flow is iso- or over-pressured it cannot collimate so it is conical with an asymptotic vanishing pressure as shown in Fig. 8c. Even if it is under-pressured at the base but with vanishing pressure or becoming over-pressured asymptotically as shown in Fig. 8b the cylindrical collimation is very loose because it is due only to the presence of a weak magnetic field. Conversely, if the pressure remains strong all the way it can refocalize strongly the jet and squeeze it as in Fig. 8d). In fact this last situation looks like a stopped jet somehow.

5.2 Application to the classification

We found that the asymptotic morphology of the outflow is controlled by the efficiency of the magnetic rotator and the pressure gradient across the streamlines, Eq. (3). The same model shows interesting jet solutions in relation with the various flows seen in AGN (Fig. 8), so we can try to use it in understanding their taxonomy. The efficiency of the magnetic rotator is related to the magnetic properties of the central object in the AGN and/or its disk while the pressure gradient is related to the pressure variation across the streamlines. We may assume that this can be somehow related to the environment through which the jet propagates (this is of course an extra assumption to the model itself). Thus, we may discuss the following possibilities in the framework of the classification scheme of AGN shown in Fig. 2, as they are summarized in Table 1 (this scheme is also shown on the top of Fig 8). In this classification, we move from Type 2 to Type 0 because of orientation effects, as we already discussed. The new interesting element is that a classification from one class to another results now as the efficiency of the magnetic rotator and the environment change.

Table 1. AGN classification according to orientation and efficiency of magnetic rotator

Radio-emission (Type: 2, 1, 0)	Magnetic Rotator, ϵ	Collimation, ϵ'
Quiet (Sey.2, Sey.1, BAL & QSO)	Inefficient, $\epsilon \ll 0$	Weak, $\epsilon' \lesssim 0$
Loud (FR I, BL Lac)	Intermediate effic., $\epsilon \sim 0$	Good, $\epsilon' \gtrsim 0$
Loud (FR II, BLRG & SSRQ, FSRQ)	Efficient, $\epsilon > 0$	Tight, $\epsilon' > 0$

(I). *Inefficient magnetic rotators*, $\epsilon \lesssim 0$, corresponding to radio-quiet AGN (Seyferts, etc. . .) with uncollimated or, loosely collimated outflows. One possibility is that $\epsilon' < 0$ such that the AGN produces a radially expanding outflow (Fig. 8c). This may happen if the source is in a rich environment such that latitudinally we have an over-pressured outflow $\mu > 0$. The other possibility is that $\epsilon' \gtrsim 0$, i.e. ϵ' is marginally positive such that the AGN produces a ‘weakly’ collimated jet, i.e., collimation occurs slowly at large distances (Fig. 8b). This may happen, for instance, if we have a latitudinally under-pressured outflow, $\mu > 0$. Hence, if the central source is an IMR ($\epsilon \lesssim 0$) the density drops quite rapidly with the radial distance and this could be related to the weaker outflows in Seyfert 1 and 2 galaxies and radio-quiet QSO’s. We cannot exclude that in this case if pressure does not drop rapidly enough we have a stopped jet like in (Fig. 8d) with a shock at the refocalizing point, as it has been suggested for Seyferts (e.g. [82]).

(II). *Efficient magnetic rotators*, $\epsilon > 0$, corresponding to radio-loud AGN of high luminosity with well collimated and powerful jets (FR II, etc...). In this case, since ϵ obtains high positive values, we have a tightly collimated jet (Fig. 8a), regardless of the value of μ , i.e., regardless if the jet propagates in a rich or poor environment.

(III). *Intermediate efficiency magnetic rotators*, $\epsilon' > 0$, corresponding to radio-loud AGN of low luminosity (FR I, etc...) with collimated jets. The two possibilities are either that ϵ is marginally positive and $\mu < 0$, or, ϵ is marginally negative and $\mu > 0$. In this case, we always have $\epsilon' > 0$ and hence the outflows always have asymptotically cylindrical flux tubes. Note also that many extragalactic jets, as deduced from X-ray data on the hot surrounding plasma, seem to be propagating in rich environments [39]. For example, this seems to be the case with FRI type of Radio Galaxies [80].

If the strength of the magnetic rotator reduces, one expects a smooth transition from a jet to a loosely collimated wind and finally to a radial wind. This would correspond to moving from the radio-loud quasars and Blazars of Fig. 2 to the radio-quiet Seyfert galaxies and QSO's. The same transition would be true if the closeby environment, possibly the corona of the central engine, becomes more and more dense. This is also consistent with the different kinds of parent galaxies: early-type (with very low density interstellar gas) for radio-loud AGN, Blazars, QSO, and spiral galaxies for Seyferts.

Despite that the model on which our conclusions are based is clearly nonrelativistic, we conjecture that its basic trends should be preserved in relativistic cases as well if we rely on previous relativistic extensions of non relativistic results [33]. However, collimation of relativistic winds from a spherical source (see [16]) seems rather difficult to achieve because the plasma has a very high effective density in this case (something that somehow fits into the criterion for collimation we previously discussed). This can be solved in two ways. Either, the jet is launched almost along its rotational axis as it is usually done in numerical simulations of relativistic disk winds, or, there is in fact an indication that the relativistic pair plasma beam is confined by an heavier more extended hadronic component which is not relativistic or only mildly (cf. [46]).

6 Concluding remarks

In this review we started with a long catalogue of the taxonomy of outflows from AGN and μ Quasars but soon we realized that all such outflows share common characteristics that can be understood in physical terms.

First, magnetic collimation of winds into jets appears to be a rather general property of the MHD equations governing plasma outflows (the hoop stress paradigm) and is likely to survive to the instabilities of the toroidal magnetic field, although such instabilities indeed must be present and can

deeply modify the morphology of the outflow. Pressure gradients also contribute to confine the outflows in addition to toroidal magnetic fields. In extragalactic jets and on scales of several kpc, pressure confinement by the environment seems to be present especially in the less luminous and less collimated ones, while close to the center the jet may be either magnetically or thermally confined.

Second, the transformation of magnetocentrifugal energy into kinetic energy seems to be a natural driving mechanism for outflows from black hole magnetospheres and accretion disks, but the presence of very hot coronae in AGN and the necessity along the rotational axis to have a thermal driving indicates that the contribution from the thermal energy is essential if not dominant, with appropriate heating processes occurring in the plasma.

And third, the jet composition is likely to be made of both electron/positron pairs and electrons/protons, the first being more likely to be extracted from the central magnetosphere while the second from the more extended corona and surrounding disk.

The MHD acceleration/collimation mechanisms can work in very different astrophysical scenarios, whenever we have a rotating magnetized body such as a supermassive black hole surrounded by an accretion disk. Even though the basic thermal/magnetic driving and confining mechanisms discussed here should be qualitatively valid also for relativistic velocities, more detailed modeling of such relativistic jets from AGN is needed at this point. However a consistent modeling of jets in AGN requires the crossing of all MHD singularities. And we have seen how difficult it is to solve the steady equations and how important it is for putting carefully the boundary conditions in numerical simulations. At this point the analogy of horizon/limiting characteristics and ergosphere/elliptic-hyperbolic-transitions may be of some help in the future as there is already a long experience in numerical simulations of black holes and how to tackle with this difficulty.

Finally, we have reviewed the standard unification scheme of AGN. The fact that some classes of objects transform into other classes with the viewing angle, seems to be basically secure by now. And, in this article we added that there is a physical criterium separating the various classes among themselves. We see that the degree of collimation does not depend only on the spin of the central black hole or the fueling or the composition of the environment, but in a subtle composition of all these processes which can be expressed in terms of the energetic distribution. In this sense it allows to reconcile the different scenarios proposed to explain the taxonomy of winds and jets around compact objects, in particular the FRII/FRI dichotomy.

References

1. Antonucci, R., *ARA&A*, **31**, 473-521 (1993)
2. Bardeen, J. M., Berger, B.K., *ApJ*, **221**, 105-113 (1978)

3. Baum, S.A., Zirbel, E.I., O’Dea, C.P., *ApJ*, **451**, 88-99 (1995)
4. Begelman, M.C., *ApJ*, **493**, 291-300 (1998)
5. Beskin, V. S., Okamoto, I., *MNRAS*, **313**, 445-453 (2000)
6. Blandford, R.D., in *Active Galactic Nuclei*, eds. T.J.-L. Courvoiser and M. Mayor, Springer, Berlin, pp. 161-275 (1990)
7. Blandford, R. D., Begelman, M.C., *MNRAS*, **303**, L1-L5 (1999)
8. Blandford, R. D., Levinson, A., *ApJ*, **441**, 79-95 (1995)
9. Blandford, R. D., in *Astrophysical Discs - An EC Summer School*, Astronomical Society of the Pacific, Conference series Vol. 160, eds. J. A. Sellwood and J. Goodman, p. 265., *AstroPh* 9902001 (1999)
10. Blandford, R. D., in *Magnetic Activity in Stars, Discs and Quasars*, eds. D. Lynden-Bell, E. R. Priest and N. O. Weiss., *Phil. Trans. Roy. Soc. A*, astro-ph 0001499 (2000)
11. Blandford, R.D., Payne, D.G., *MNRAS*, **199**, 883-903 (1982)
12. Blandford, R.D., Rees, M.J., *MNRAS*, **169**, 395-415 (1974)
13. Blandford, R.D., Znajek, R.L., *MNRAS*, **179**, 433-456 (1977)
14. Bodo, G., Rossi, P., Massaglia, S., Ferrari, A., Malagoli, A., Rosner, R., *A&A*, **333**, 1117-1129 (1998)
15. Bogovalov, S.V., *A&A*, **323**, 634-643 (1997)
16. Bogovalov, S.V., Tsinganos, K., *MNRAS*, **305**, 211-224 (1999)
17. Breitmose, E., Camenzind, M., *A&A*, **363**, 207-225 (2000)
18. Brunthaler, A., et al., *A&A*, **357**, L45-L48 (2000)
19. Camenzind, M., in *Solar and Astrophysical Magnetohydrodynamic Flows*, ed. K.C. Tsinganos, Kluwer (Dordrecht), p. 699-725 (1996)
20. Camenzind, M., in *Astrophysical Jets: Open Problems*, eds. G. Bodo, and S. Massaglia, Gordon and Breach Science Pubs., pp. 3-29 (1998)
21. Capetti, A., Trussoni, E., Celotti, A., Feretti, L., Chiaberge, M., *MNRAS*, **318**, 493-500 (2000)
22. Carter, B., in *Black Holes*, eds. C. DeWitt, and B.S. DeWitt, Gordon and Breach Science Pubs., pp. 57-214 (1972)
23. Casse, F., Ferreira, J., *A&A*, **353**, 1115-1128 (2000a)
24. Casse, F., Ferreira, J., *A&A*, **361**, 1178-1190 (2000b)
25. Celotti, A., in *Astrophysical Jets: Open Problems*, eds. G. Bodo, and S. Massaglia, Gordon and Breach Science Pubs., pp. 79-85 (1998)
26. Chan, K.L., Henriksen, R.H., *ApJ*, **241**, 534-551 (1980)
27. Cheng, A.Y.S., O’Dell, S.L., *ApJ*, **251**, L49-L54 (1981)
28. Chiaberge, M., Celotti, A., Capetti, A., *A&A*, **349**, 77-87 (1999)
29. Chiaberge, M., Celotti, A., Capetti, A., Ghisellini, G., *A&A*, **358**, 104-112 (2000)
30. Contopoulos, J., *ApJ*, **450**, 616-627 (1995)
31. Contopoulos, J., Lovelace, R.V.E., *ApJ*, **429**, 139-152 (1994)
32. Corbel, S., Fender, R.P., Tzioumis, A.K., Nowak, M., McIntyre, V., Durouchoux, P., Sood, R., *A&A*, **359**, 251-268 (2000)
33. Chiueh, T., Li, Z.-Y., Begelman, M.C., *ApJ*, **377**, 462-466 (1991)
34. Das, T.K., *MNRAS*, **318**, 294-302 (2000)
35. Dhawan, V., Mirabel, I.F., Rodríguez, L.F., *ApJ*, **543**, 373-385 (2000)
36. Fabian, A. C., Rees, M. J., *MNRAS*, **277**, L55-L58 (1995)
37. Fendt, C., Camenzind, M., Appl, S., *A&A*, **300**, 791-807 (1995)
38. Fender, R.P., in “Astrophysics and Cosmology : a collection of critical thoughts”, springer Lecture notes in Physics, (2000) astro-ph9907050

39. Feretti, L., Fanti, R., Parma, P., Massaglia, S., Trussoni, E., Brinkmann, W., *A&A*, **298**, 699-710 (1995)
40. Ferreira, J., *A&A*, **319**, 340-359 (1997)
41. Ghisellini, G., Bodo, G., Trussoni, E., Rees, M.J., *ApJ*, **362**, L1-L4 (1990)
42. Ghisellini, G., Bodo, G., Trussoni, E., *ApJ*, **401**, 87-98 (1992)
43. Gopal-Krishna, Wiita, P.J., *A&A*, **363**, 507-516 (2000)
44. Hanasz M., Sol H., Sauty C., *MNRAS*, **316** (3), 494-506 (2000)
45. Heinz, J., Begelman M.C., *ApJ*, **535**, 104-111 (2000)
46. Henri, G., Pelletier, G., *ApJ*, **383**, L7-L10 (1991)
47. Heyvaerts, J., Norman, C.A., *ApJ*, **347**, 1055-1081 (1989)
48. Kim, W.-T., Ostriker, E.C., *ApJ*, **540**, 372-403 (2000)
49. Krasnopolsky, R., Li, Z.-Y., Blandford, R., *ApJ*, **526**, 631-642 (1999)
50. Kersalé, E., Longaretti, P.-Y., Pelletier, G., *A&A*, **363**, 1166-1176 (2000)
51. Keppens, R., Goedbloed, J.P., *ApJ*, **530**, 1036-1048 (2000)
52. Koide, S., Shibata, K., Kudoh, T., *ApJ*, **495**, L63-L66 (2000)
53. Königl, A., Kartje, J.F., *ApJ*, **434**, 446-467 (1994)
54. Königl, A., Wardle, M., *MNRAS*, **279**, L61-L64 (1996)
55. Koide, S., Meier, D.L., Shibata, K., *ApJ*, **536**, 668-674 (2000)
56. Kudoh, T., Matsumoto, R., Shibata, K., *ApJ*, **508**, 186-199 (1998)
57. Lery, T., Henriksen R. N., Fiege J., *A&A*, **350**, 254-274 (1999)
58. Lery, T., Heyvaerts, J., Appl, S., Norman, C.A., *A&A*, **347**, 1055-1068 (1998)
59. Lery, T., Frank, A., *ApJ*, **533**, 897-910 (2000)
60. Lery, T., Baty, H., Appl, S., *A&A*, **355**, 1201-1208
61. Li Z-Y., Chiueh, T., Begelman, M.C., *ApJ*, **394**, 459-471 (1992)
62. Li, Z-Y., *ApJ*, **444**, 848-860 (1995)
63. Li, Z-Y., *ApJ*, **465**, 855-868 (1996)
64. Livio, M., *PhR*, **311**, 225-251 (1999)
65. Livio, M., Ogilvie, G.I., Pringle, J.E., *ApJ*, **512**, 100-104 (1999)
66. Lister, M.L., Smith, P.S., *ApJ*, **541**, 66-87 (2000)
67. Michel, F.C., *ApJ*, **158**, 727-738 (1969)
68. Mirabel, I.F., Rodríguez, L.F., *ARA&A*, **37**, 409-443 (1999)
69. Nitta, S-Y., *MNRAS*, **284**, 899-910 (1997)
70. Nobuta, K., Hanawa, T., *ApJ*, **510**, 614-630 (1999)
71. O'Dell, S.L., *ApJ*, **243**, L147-L149 (1981)
72. Okamoto, I., *MNRAS*, **307**, 253-278 (1999)
73. Okamoto, I., *MNRAS*, **318**, 250-262 (2000)
74. Ostriker, E.C., *ApJ*, **486**, 291-306 (1997)
75. Ouyed, R., Pudritz, R.E., *ApJ*, **482**, 712-732 (1997)
76. Parker, E.N., *Interplanetary Dynamical Processes*, Interscience, New York (1963)
77. Pietrini, P., Torricelli-Ciamponi, G., *A&A*, **363**, 455-475 (2000)
78. Pelletier, G., Sol, H., *MNRAS*, **254**, 635-646 (1992)
79. Proga, D., Stone, J.M., Kallman, T.R., *ApJ*, **543**, 686-696 (2000)
80. Prestage, R.M., Peacock, J.A., *MNRAS*, **230**, 131-160 (1998)
81. Rees, M., Begelman, M., Blandford, R., Phinney, E., *Nature* **295**, 17-21 (1982)
82. Rosso, F., PhD thesis, Université de Grenoble (1994)
83. Sakurai, T., *A&A*, **152**, 121-129 (1985)
84. Sauty, C., Tsinganos, K., *A&A*, **287**, 893-926 (1994)
85. Sauty, C., Tsinganos, K., Trussoni, E., *A&A*, **348**, 327-349 (1999)

86. Schatzman, E., *Ann. Astroph.*, **25**, 18-29 (1962)
87. Shibata, K., Uchida, Y., *PASJ*, **42**, 39-67 (1990)
88. Sol, H., Pelletier, G., *MNRAS*, **237**, 411-429 (1989)
89. Sikora, M., Madejski, G., *ApJ*, **534**, 109-113 (2000)
90. Smith, E.P., Heckman, T.M., Bothum, G.D., Romanishin, W., Balick, B., *ApJ*, **306**, 64-89 (1986)
91. Spruit, H.C., Cao, X., *A&A*, **287**, 80-86 (1994)
92. Spruit, H.C., in "Evolutionary Processes in Binary Stars", eds. R.A.M.J. Wijers et al., Kluwer, Netherlands, pp. 249-286 (1996)
93. Tagger, M., Pellat, R., *A&A*, **349**, 1003-1016 (1999)
94. Trussoni, E., Sauty, C., Tsinganos, K., *A&A*, **325**, 1114 (1997)
95. Tsinganos, K., Sauty, C., Surlantzis, G., Trussoni, E., Contopoulos, J., *MNRAS*, **283**, 811-820 (1996)
96. Tsinganos, K., Bogovalov, S.V., *A&A*, **356**, 989-1002 (2000)
97. Uchida, Y., Shibata, K., *PASJ*, **37**, 515-535 (1985)
98. Urry, C.M., Padovani, P., *PASP*, **107**, 803-845 (1999)
99. Usmanov, A.V., Goldstein, M.L., Besser, B.P., Fritzer, J.M., *JGR*, **105**(A6), 12,675-12,695 (2000)
100. Ustyugova, G.V., Koldova, A.V., Romanova, M.M., Chechetkin, V.M., Lovelace, R.V.E., *ApJ*, **516**, 221-235 (1999)
101. Ustyugova, G.V., Lovelace, R.V.E., Romanova, M.M., Li, H., Colgate, S.A., *ApJ*, **541**, L21-L24 (2000)
102. Vlahakis, N., PhD thesis, University of Crete (1998)
103. Vlahakis, N., Tsinganos, K., *MNRAS*, **298**, 777-789 (1998)
104. Vlahakis, N., Tsinganos, K., Sauty, C., Trussoni, E., *MNRAS*, **318**, 417-428 (2000)
105. Wilson, A.S., Colbert, E.J.M., *ApJ*, **438**, 62-71 (1995)

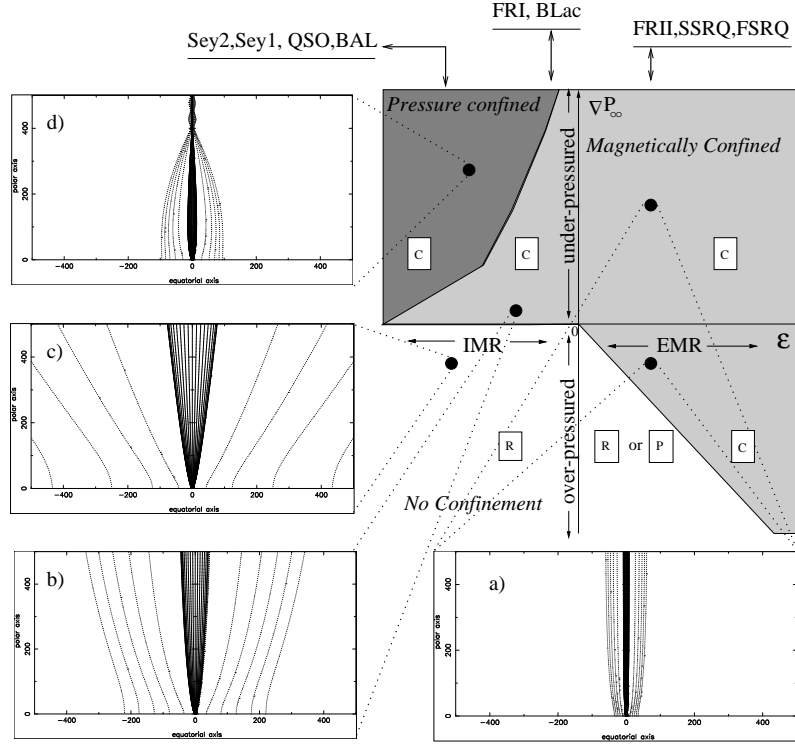


Fig. 8. Degree of collimation obtained as a function of the asymptotic transverse pressure gradient (vertical axis) and the efficiency of the magnetic rotator (horizontal axis) with typical solutions for winds in (b) and (c), jets in (a) and stopped jets in (d). EMR are on the left, IMR on the right, underpressured jets on top and overpressured flows below. “R” corresponds to the domain or radial asymptotics, “P” to paraboloidal ones and “C” to cylindrical. See text for details. After Sauty, Tsinganos and Trussoni [85].